Glycobiology vol. 19 no. 5 pp. 488–498, 2009
doi:10.1093/glycob/cwp005
Advance Access publication on February 3, 2009

Structural and functional changes of sulfated glycosaminoglycans in *Xenopus laevis* during embryogenesis

Shuhei Yamada[1,4,5], Masako Onishi[5], Reiko Fujinawa[2,5], Yuko Tadokoro[3,5], Koji Okabayashi[6], Makoto Asashima[6,7], and Kazuyuki Sugahara[4,5]

[4]Laboratory of Proteoglycan Signaling and Therapeutics, Hokkaido University Graduate School of Life Science, Sapporo 001-0021; [5]Department of Biochemistry, Kobe Pharmaceutical University, Higashinada-ku, Kobe 658-8558; [6]ICORP Organ Regeneration Project, Japan Science and Technology Agency (JST); and [7]Department of Life Sciences (Biology), Graduate School of Arts and Sciences, The University of Tokyo, Tokyo 153-8902, Japan

Received on July 9, 2008; revised on December 19, 2008; accepted on January 16, 2009

***Xenopus laevis* is an excellent animal for analyzing early vertebrate development. Various effects of glycosaminoglycans (GAGs) on growth factor-related cellular events during embryogenesis have been demonstrated in *Xenopus*. To elucidate the relationship between alterations in fine structure and changes in the specificity of growth factor binding during *Xenopus* development, heparan sulfate (HS) and chondroitin/dermatan sulfate (CS/DS) chains were isolated at four different embryonic stages and their structure and growth factor-binding capacities were compared. The total amounts of both HS and CS/DS chains decreased from the pre-midblastula transition to the gastrula stage, but increased exponentially during the following developmental stages. The length of HS chains was not significantly affected by development, whereas that of CS/DS chains increased with development. The disaccharide composition of GAGs in embryos also changed during development. The degree of sulfation of the HS chains gradually decreased with development. The predominant sulfation position in the CS/DS chains shifted from C4 to C6 of GalNAc during embryogenesis. Growth factor-binding experiments using a BIAcore system demonstrated that GAGs bound growth factors including fibroblast growth factors-1 and -2, midkine, and pleiotrophin, with comparable affinities. These affinities significantly varied during development, although the correlation between the structural alterations of GAGs and the change in the ability to bind growth factors remains to be clarified. The expression of saccharide sequences, which specifically interact with a growth factor, might be regulated during development.**

[1]To whom corresponding may be addressed: Tel: +81-(11)-706-9055; Fax: +81-(11)-706-9055; e-mail: tjohej@sci.hokudai.ac.jp
[2]Present address: RIKEN Advanced Science Institute Chemical Biology Department System Glycobiology Research Group Disease Glycomics Team, Wako, Saitama 351-0198, Japan.
[3]Present address: Division of Stem Cell Medicine, Center for Cancer and Stem Cell Research, Cancer Research Institute, Kanazawa University, Kanazawa, Ishikawa 920-0934, Japan.

Keywords: chondroitin sulfate/embryogenesis/glycosaminoglycan/heparan sulfate/*Xenopus laevis*

Introduction

During development, the formation of complex body structures is governed by several signaling factors, such as Wnt, hedgehog, midkine (MK), pleiotrophin (PTN), fibroblast growth factors (FGFs), epidermal growth factor, and members of the transforming growth factor-β superfamily. Most of these growth/differentiation factors are capable of binding to glycosaminoglycans (GAGs) such as heparan sulfate (HS) and chondroitin/dermatan sulfate (CS/DS) (Conrad 1998). A number of studies have demonstrated that some of these signaling factors exert their functions through interactions with HS chains (Perrimon and Bernfield 2000; Lin 2004).

GAGs are complex sulfated polysaccharides with a backbone structure composed of repeating disaccharide units and occur in animal tissues as proteoglycans (PGs), in which these polysaccharide chains are covalently attached to a respective core protein (Rodén 1998). PGs are found on the cell-surface and in the extracellular matrix. The highly heterogeneous sulfated patterns found in the GAG chains and the specific molecular interactions of GAGs with protein factors are involved in the regulation of various biological processes (Perrimon and Bernfield 2000; Lin 2004).

Xenopus laevis is a freshwater animal that can be induced to lay eggs repeatedly by a simple hormone injection. This useful feature, coupled with the large size of its embryos, which allow micromanipulation and microinjection, and their rapid rate of development, makes *Xenopus* an excellent model animal for analyzing early vertebrate development (Sive et al. 2000). Shortly after fertilization, rapid cleavages of *Xenopus* embryos result in the formation of the blastula. At around the midblastula stage, the cell cycle remodels from rapid embryonic cleavage cycles to longer, more regulated somatic cell cycles and gastrulation (gastrula stage) commences. This key developmental event is called the midblastula transition (MBT). After the end of gastrulation, the process of neurulation (neurula stage) occurs, during which the neural plate folds to become the neural tube. Following the closure of the neural tube, the period of organogenesis commences (tailbud stage).

Various effects of PGs on growth factor-related cellular events have been observed during *Xenopus* embryogenesis. HS-PG has been postulated to participate in the mesoderm's formation in early *Xenopus* embryos (Brickman and Gerhart 1994; Itoh and Sokol 1994; Furuya et al. 1995). Immunohistochemistry using the anti-HS mouse monoclonal antibody, HepSS-1, revealed that HS-PG occurs mainly in the animal hemisphere in the early gastrula (Furuya et al. 1995). Furthermore, elimination of HS-PGs by heparitinases induced abnormal mesodermal differentiation

(Brickman and Gerhart 1994; Itoh and Sokol 1994; Furuya et al. 1995). PGs appear to play indispensable roles in *Xenopus* development by modifying actions of GAG-binding growth factors and morphogens. Specific antisense knock-down of *Xenopus* heparanases, HS-degrading enzymes, results in a failure of embryogenesis to proceed, suggesting that heparanases regulate the developmental processes (Bertolesi et al. 2008). The serine protease xHtrA1 activates FGF signals by cleaving the core proteins of PGs and releasing cell-surface GAG-bound FGF ligands (Hou et al. 2007). CS-PGs also play an important role in *Xenopus* embryos. The notochord-derived CS-PGs act as repulsive signaling molecules that are recognized by contactin, which has been implicated in axonal guidance of spinal sensory neurons in *Xenopus* tailbud embryos (Fujita and Nagata 2005).

Nurcombe et al. (1993) reported, although it was not confirmed by others, that a single species of HS-PG undergoes a rapid, tightly controlled change in growth factor-binding specificity concomitant with the temporal expression of FGF-1 and FGF-2 during murine neural development. The *Xenopus* GAG chains may also undergo dynamic structural changes and switch binding properties coordinated with the timing of the expression of various growth/differentiation factors such as FGF-2, MK, and PTN to control their activities during early embryogenesis. However, this concept has never been established.

In *Xenopus* development, the expression of several GAG-interacting growth/differentiation factors has been detected. Growth factors belonging to the FGF family are involved in morphological events during embryogenesis in *Xenopus*. The expression of FGF-2 is turned on from anterior and posterior regions simultaneously at the mid-neurula stage and greatly increases during the late neurula and tailbud stages (Song and Slack 1994). Disruption of the FGF-2 signaling pathway resulted in severe inhibition of invagination and neural tube closure in the posterior region of *Xenopus* embryos (Amaya et al. 1991). MK was first expressed at the mid-gastrula stage and was located in the neural anlage at the late gastrula stage (Sekiguchi et al. 1995). At the neurula and tailbud stages, MK was predominantly localized in the brain and neural tube. The expression of PTN was restricted to the central nervous system, particularly in the hindbrain at the tailbud stage in *Xenopus* (Tujimura et al. 1995).

In this study, we have characterized *Xenopus* HS and CS/DS at four different embryonic stages, the pre-MBT, gastrula, neurula, and tailbud stages. Structure and growth factor-binding capacities were compared to elucidate the relationship between the fine structural alteration and the changes in the growth factor-binding specificities during development using FGF-1, FGF-2, MK, and PTN as representative growth/differentiation factors.

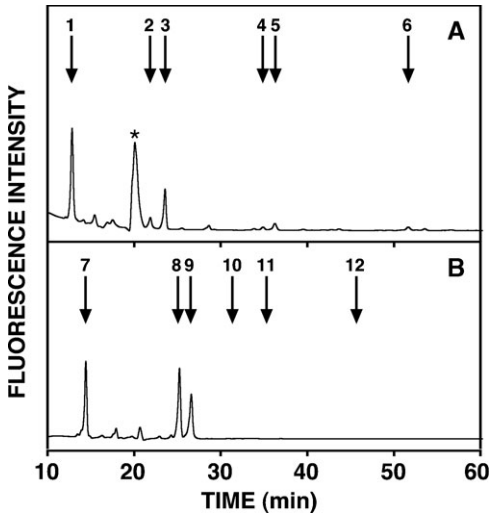

Fig. 1. Disaccharide composition analysis of HS (**A**) and CS/DS (**B**) chains from *Xenopus* embryos at the tailbud stage. The GAG fraction prepared from *Xenopus* embryos at the tailbud stage (2.4 mg as the dried material) was digested with chondroitinase ABC or a mixture of heparinase and heparitinase. Each digest was labeled with the fluorophore 2AB and analyzed by HPLC on an amine-bound silica column. The peak eluted at around 20 min and marked by an *asterisk* is due to an unidentified impurity derived from the enzyme solution or the 2AB reagent. The elution positions of authentic 2AB-disaccharide standards derived from HS and CS/DS are indicated by numbered arrows in panels A and B, respectively: (1) ΔHexUA-GlcNAc; (2) ΔHexUA-GlcNAc(6S); (3) ΔHexUA-GlcNS; (4) ΔHexUA-GlcNS(6S); (5) ΔHexUA(2S)-GlcNS; (6) ΔHexUA(2S)-GlcNS(6S); (7) ΔDi-0S; (8) ΔDi-6S; (9) ΔDi-4S; (10) ΔDi-diS_D; (11) ΔDi-diS_E; (12) ΔDi-triS.

Results

Structural analysis of Xenopus GAGs from different developmental stages

The GAG fractions purified at different developmental stages were digested exhaustively with chondroitinase ABC or a mixture of heparinase and heparitinase, and the resulting disaccharides were labeled with a fluorophore 2-aminobenzamide (2AB) and analyzed by HPLC on an amine-bound silica column. As representative chromatograms, the HPLC profile of the GAG fraction from the tailbud stage digested with chondoritinase ABC or a mixture of heparinase and heparitinase is shown in Figure 1. Each disaccharide peak was identified by comparison of the elution position with those of the standard 2AB-disaccharides. The yield of each disaccharide was calculated based on the fluorescence intensity (Kinoshita and Sugahara 1999). The total amounts and composition of disaccharides of the CS/DS and HS produced from *Xenopus* embryos at different

Table I. Composition of unsaturated disaccharides produced from HS in *Xenopus* embryos at the different developmental stages[a]

	Unsaturated disaccharide (%)							
	ΔHexUA-GlcNAc	ΔHexUA-GlcNS	ΔHexUA-GlcNAc(6S)	ΔHexUA-GlcNS(6S)	ΔHexUA(2S)-GlcNS	ΔHexUA(2S)-GlcNS(6S)	Sulfate/disaccharide[b]	Total amount in the dried materials (ng/mg)
Pre-MBT	34 ± 2.2	20 ± 1.4	10 ± 1.4	5 ± 1.3	19 ± 3.7	12 ± 1.8	1.14	4.7
Gastrula	41 ± 0.3	25 ± 1.3	20 ± 1.7	1 ± 0.1	8 ± 0.5	5 ± 0.2	0.78	1.6
Neurula	45 ± 2.3	26 ± 6.0	7 ± 1.4	5 ± 3.4	12 ± 1.8	5 ± 1.8	0.82	18.2
Tailbud	65 ± 4.6	20 ± 0.8	4 ± 0.9	2 ± 0.3	7 ± 1.5	2 ± 1.2	0.48	92.7

[a]The values are expressed as the mean ± range for two independent experiments.
[b]The average number of sulfate groups/disaccharide unit is given.

Table II. Composition of unsaturated disaccharides produced from CS/DS in *Xenopus* embryos at the different developmental stages[a]

	Unsaturated disaccharide (%)					Sulfate/ disaccharide[b]	Total amount in the dried materials (ng/mg)	Ratio	
	ΔDi-0S	ΔDi-4S	ΔDi-6S	ΔDi-diS$_D$	ΔDi-diS$_E$			HS/(CS+DS)	DS/(CS+DS)[c]
Pre-MBT/ABC+AC-I	10 ± 0.8	79 ± 2.2	11 ± 1.4	ND[d]	ND	0.90	4.1	1.1	0.55
Pre-MBT/AC-I	7	32	6						
Gastrula/ABC+AC-I	24 ± 2.4	72 ± 0.9	4 ± 1.5	ND	ND	0.76	0.52	3.1	0.32
Gastrula/AC-I	24	41	3						
Neurula/ABC+AC-I	15 ± 1.0	58 ± 1.3	27 ± 0.4	ND	ND	0.85	7.6	2.4	0.29
Neurula/AC-I	13	32	26						
Tailbud/ABC+AC-I	33 ± 1.4	23 ± 2.0	44 ± 0.6	ND	ND	0.67	73.7	1.3	0.23
Tailbud/AC-I	24	11	42						

[a]*Xenopus* GAG fractions were extensively digested with a mixture of chondroitinases ABC and AC-I or chondroitinase AC-I alone. Percent recoveries of disaccharides obtained by digestion were calculated based on the peak area in the HPLC chromatograms and are expressed in molar proportions taking the total amount obtained by digestion with a mixture of chondroitinases ABC and AC-I as 100%. The values for the digest with a mixture of chondroitinases ABC and AC-I are expressed as the mean ± range for two independent experiments.
[b]The average number of sulfate groups/disaccharide unit is given.
[c]The amount of DS was calculated as follows: the amount of disaccharides released by a mixture of chondroitinases ABC and AC-I minus the amount of disaccharides released by chondroitinase AC-I.
[d]ND, not detected.

developmental stages are summarized in Tables I and II as well as in Figures 2 and 3. The total amounts of both HS and CS/DS chains decreased from the pre-MBT to the gastrula stage, but then increased exponentially during the following developmental stages. The zygotic genome in *X. laevis* is quiescent until the MBT stage, and transcription is repressed at the pre-MBT stage. Thus, GAG synthesis during the pre-MBT stage is regulated by maternal transcripts and proteins. The change in the total amount of GAGs in *Xenopus* embryos at around the gastrula stage and thereafter probably reflects the switchover of GAG biosynthetic enzymes from maternal to zygotic gene products. The dramatic increase in GAGs at the tailbud stage may indicate the requirement of large amounts of GAGs for *Xenopus* organogenesis at this stage.

Reproducible differences were detected in the disaccharide profile of HS and CS/DS from *Xenopus* embryos at different developmental stages. The major disaccharide unit in the HS fractions was the nonsulfated disaccharide ΔHexUAα1-

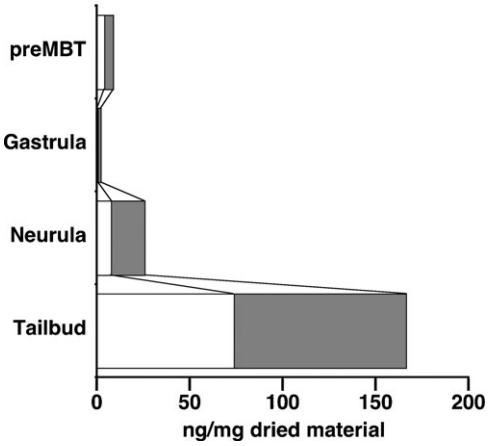

Fig. 2. The total amount of GAGs from *Xenopus* embryos at the different developmental stages. The yields of HS and CS/DS from embryos at the different developmental stages were calculated based on the fluorescence intensity of the peaks detected by HPLC. Hatched and open areas in each bar indicate HS and CS/DS, respectively.

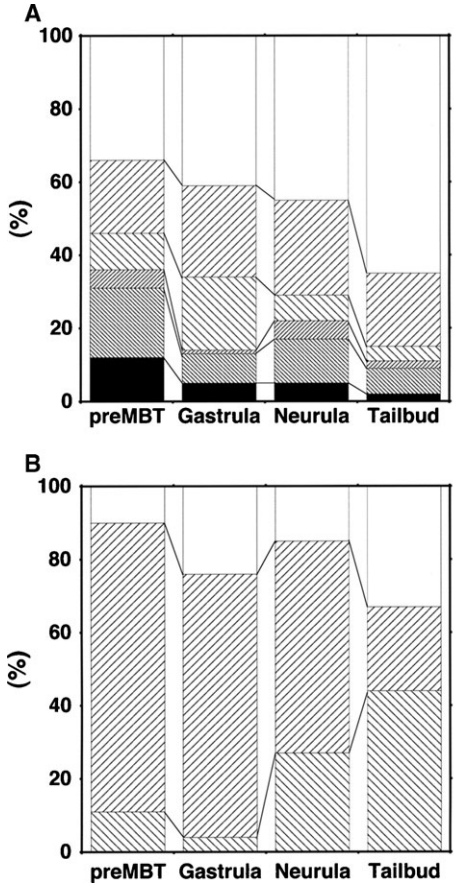

Fig. 3. Comparison of disaccharide composition of *Xenopus* HS (**A**) and CS/DS (**B**) at different developmental stages. The structures of the *Xenopus* HS and CS/DS are illustrated based on the findings obtained from the analysis of the disaccharide composition (Figure 1 and Tables I and II). The width of each box corresponds to the proportion of each disaccharide unit. The variously shaded boxes for the repeating disaccharide region of HS (panel A) indicate ΔHexUA-GlcNAc, ΔHexUA-GlcNS, ΔHexUA-GlcNAc(6S), ΔHexUA-GlcNS(6S), ΔHexUA(2S)-GlcNS, and ΔHexUA(2S)-GlcNS(6S), respectively, from the top. Boxes for the repeating disaccharide region of CS/DS (panel B) indicate ΔDi-0S, ΔDi-4S, and ΔDi-6S, respectively, from the top. Note that boxes for the repeating disaccharide region represent the composition, but do not reflect the location or clustering of the disaccharide units along the polysaccharide chains.

4GlcNAc at all stages tested. There was an increase in the proportion of the nonsulfated disaccharide and a decrease in the sulfated disaccharide units with development. The average number of sulfate groups/100 disaccharides in the HS preparations from the pre-MBT, gastrula, neurula, and tailbud stages was 114, 78, 82, and 48, respectively.

The complete digestion of *Xenopus* GAG fractions with chondroitinase ABC yielded the disaccharides, ΔHexUAα1-3GalNAc (ΔDi-0S), ΔHexUAα1-3GalNAc(4-sulfate) (ΔDi-4S), and ΔHexUAα1-3GalNAc(6-sulfate) (ΔDi-6S). The proportions of ΔDi-0S and ΔDi-6S increased, whereas that of ΔDi-4S decreased gradually with development. Oversulfated disaccharide units such as ΔHexUA(2-sulfate)α1-3GalNAc(6-sulfate) and ΔHexUAα1-3GalNAc(4,6-disulfate) found in vertebrate CS (Ueoka et al. 2000; Tsuchida et al. 2001; Maeda et al. 2003; Bao et al. 2004; Bergefall et al. 2005; Mitsunaga et al. 2006) were not detected at any developmental stages.

The molecular sizes of the *Xenopus* HS and CS/DS chains at different developmental stages were analyzed by gel filtration chromatography on a column of Superdex 200. To monitor small amounts of GAGs, aliquots of individual fractions were lyophilized and digested with chondroitinase ABC or a mixture of heparinase and heparitinase, respectively, and then the products were derivatized with a fluorophore 2AB and analyzed by anion-exchange HPLC as described in *Materials and methods*. Since the amount of the GAG fraction from the pre-MBT stage was limited, the molecular size of GAGs at this stage was not analyzed. Compared with the calibration plot prepared using size-defined commercial polysaccharides, the average molecular size of the major component in the *Xenopus* HS and CS/DS at the gastrula, neurula, or tailbud stage was estimated to be 47, 47, or 57, and 47, 68, or 83 kDa, respectively (Figure 4). The chain length of *Xenopus* HS fractions did not significantly change during development, whereas that of *Xenopus* CS/DS fractions increased with development. It should also be noted that the chain length of *Xenopus* CS/DS preparations was rather heterogeneous.

The proportion of the DS structure in *Xenopus* CS/DS chains was also analyzed. GAG preparations were extensively digested with a mixture of chondroitinases ABC and AC-I or chondroitinase AC-I alone, and the resultant unsaturated disaccharides were individually analyzed by anion-exchange HPLC for identification and quantification. The linkages susceptible to chondroitinase ABC or AC-I correspond to the amounts of GlcUA and IdoUA (CS and DS) or GlcUA (CS), respectively. The data obtained from digestion experiments with chondroitinases are summarized in Table II. The proportion of the DS structure in *Xenopus* CS/DS preparations decreases during embryonic development as follows: 55 (pre-MBT), 32 (gastrula), 29 (neurula), and 23% (tailbud).

Xenopus GAGs from different developmental stages showed diverse specificity in the binding to human recombinant growth factors

To examine whether *Xenopus* GAG fractions from different developmental stages bind to growth factors in a similar or different manner, we investigated the molecular interaction of the *Xenopus GAG* samples with recombinant growth factors, FGF-1, FGF-2, MK, and PTN. Since *Xenopus* growth factors were not commercially available, human counterparts were used in this study. The kinetic parameters for the binding of recombinant growth factors to the *Xenopus* GAGs were analyzed using a surface plasmon resonance biosensor, BIAcore J, which uses a dual-channel flow and detection system to enhance the specificity of analyte detection. To analyze the interactions between *Xenopus* HS chains and growth factors, biotinylated GAG fractions were immobilized on the streptavidin-coated surface of the sample cells and the reference cells were coated with the digests of biotinylated *Xenopus* GAG fractions obtained with a mixture of heparinase and heparitinase. For the analysis of *Xenopus* CS/DS interactions, HS lyase-treated samples were immobilized on the streptavidin-coated sample cell surface and their chondroitinase ABC digests were prepared on the reference cells. Varying concentrations of individual growth factors were injected onto the sensor's surface and the interactions were analyzed. Figures 5 and 6 represent overlays of the sensorgrams for the binding of FGF-1, FGF-2, MK, and PTN to the *Xenopus* HS and CS/DS, respectively. Since the amount of the *Xenopus* GAG fraction at the pre-MBT stage was limited, the interaction experiments for the *Xenopus* CS/DS at this stage were not performed. Representative model fittings overlaid with the sensorgrams for the binding of FGF-2 to *Xenopus* HS are shown in Figure 7. The other model fittings are depicted in supplementary Figures 1 to 5.

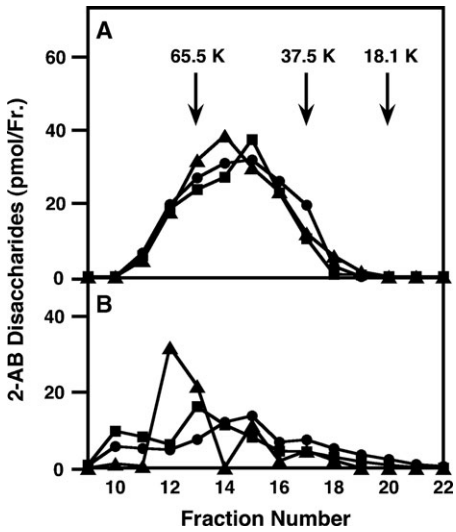

Fig. 4. Analysis of the molecular sizes of *Xenopus* HS (**A**) and CS/DS (**B**) by gel filtration chromatography. The *Xenopus* GAG fraction (160 or 75 pmol as total HS or CS/DS disaccharides, respectively) was subjected to gel filtration chromatography on a Superdex 200 column. The digests of individual fractions obtained with chondroitinase ABC or a mixture of heparinase and heparitinase was derivatized with 2AB, and then analyzed by HPLC. The amounts of the 2AB derivatives of unsaturated disaccharides were calculated based on fluorescence intensity. The circles, squares, and triangles indicate the elution profiles of the *Xenopus* HS or CS/DS from gasturula, neurula, and tailbud stage embryos, respectively. Arrows indicate the elution positions of size-defined commercial polysaccharides (Yamada et al. 2002).

The kinetic parameters, the association rate constant (k_a), the dissociation rate constant (k_d), and the equilibrium dissociation constant (K_d), for the binding of FGF-2, MK, and PTN to the *Xenopus* HS and CS/DS, are presented in Tables III and IV. These growth factors displayed K_d values in the low nM range, suggesting high affinity and a physiological significance of the interactions. The kinetic parameters for the binding of FGF-1

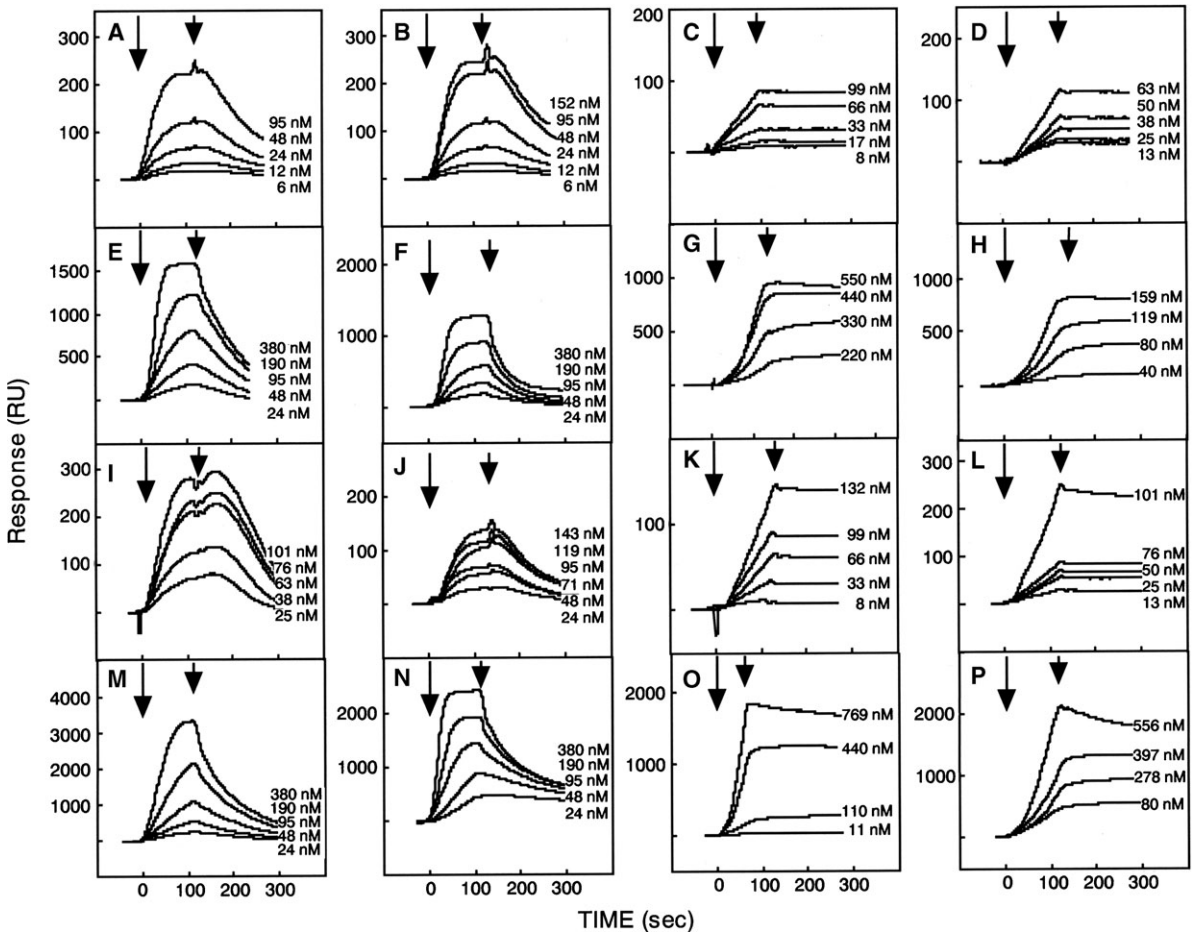

Fig. 5. Sensorgrams for the binding of FGF-1, FGF-2, MK, and PTN to *Xenopus* HS at the different developmental stages. Various concentrations of FGF-1 (**A**, **E**, **I**, **M**), FGF-2 (**B**, **F**, **J**, **N**), MK (**C**, **G**, **K**, **O**), and PTN (**D**, **H**, **L**, **P**) were injected over sensor chips immobilized with *Xenopus* embryonic HS chains prepared at the pre-MBT (**A**, **B**, **C**, **D**), gastrula (**E**, **F**, **G**, **H**), neurula (**I**, **J**, **K**, **L**), and tailbud (**M**, **N**, **O**, **P**) stages. The long arrows indicate the beginning of the association phase initiated by the injection of varying concentrations of the growth factors, and short arrows indicate the beginning of the dissociation phase initiated with the running buffer.

are not shown, since the model calculated did not fit with the real sensorgrams completely. However, the data of the binding of FGF-1 to *Xenopus* GAGs can be used qualitatively.

Both CS/DS and HS chains of *Xenopus* bound FGF-1, FGF-2, MK, and PTN with comparable affinities. To compare the affinities of growth factors for *Xenopus* GAG fractions, on rates (k_a) and off rates (k_d) were plotted on an on-/off-rate map (Figure 7). The k_d values were plotted on the *x*-axis. The further to the left a data point appears on the map, the more stable the binding is. The k_a values were plotted on the *y*-axis. The higher up, the better the recognition is. As the affinity is the ratio of the k_d value to the k_a value, growth factors binding to the GAGs with a similar affinity lie on the straight diagonal line as indicated in Figure 8. Growth factors that bind with high affinity appear in the upper-left-hand corner of the map.

Comparison of the affinity of growth factors to Xenopus HS preparations from different developmental stages

The alteration of the K_d values observed for the interaction of various growth factors with the *Xenopus* HS during development is shown in Figure 8 and Table III. No significant correlation was observed between developmental progress and variations in the binding affinity. The K_d values for the interaction of FGF-2 with the *Xenopus* HS changed as follows: 9 (pre-MBT), 760 (gastrula), 130 (neurula), and 61 nM (tailbud) (Table III and Figure 8). The affinity for FGF-2 decreased from the pre-MBT to the gastrula stage but increased at the neurula and tailbud stages. The affinities of the *Xenopus* HS for other growth factors also fluctuated with development. This pattern of fluctuation did not parallel that for *Xenopus* CS/DS as described below.

Although K_d values for the interaction of FGF-2 and PTN with *Xenopus* HS chains did not show a significant difference from the neurula to the tailbud stage, both k_a and k_d values for the corresponding interaction increased (Table III). As indicated in Figure 8, symbols for FGF-2 (open squares) and PTN (open triangles) shifted parallel to the straight diagonal lines toward the upper-right corner from the neurula to the tailbud stage (no. 3 to 4). The k_a values for the binding of FGF-2 and PTN to the tailbud stage HS were 15- and 4.3-fold higher, respectively, than those for the binding to the neurula stage HS. The k_d values for the dissociation of FGF-2 and PTN from the tailbud stage HS were 7.1- and 7.5-fold higher, respectively, than those for the dissociation from the neurula stage HS. Thus, development from

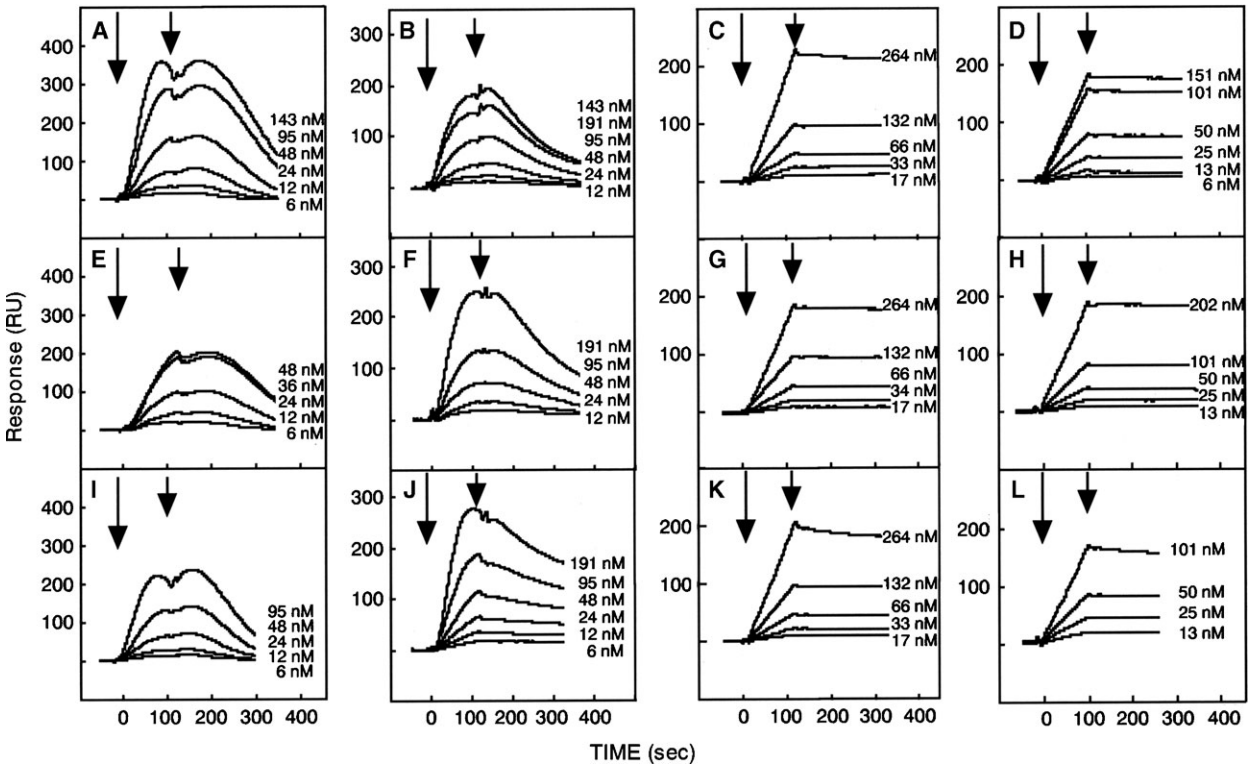

Fig. 6. Sensorgrams for the binding of FGF-1, FGF-2, MK, and PTN to *Xenopus* CS/DS at the different developmental stages. Various concentrations of FGF-1 (**A**, **E**, **I**), FGF-2 (**B**, **F**, **J**), MK (**C**, **G**, **K**), and PTN (**D**, **H**, **L**) were injected over sensor chips immobilized with *Xenopus* embryonic CS/DS chains prepared at the gastrula (**A**, **B**, **C**, **D**), neurula (**E**, **F**, **G**, **H**), and tailbud (**I**, **J**, **K**, **L**) stages. The long arrows indicate the beginning of the association phase initiated by the injection of varying concentrations of the growth factors, and short arrows indicate the beginning of the dissociation phase initiated with the running buffer.

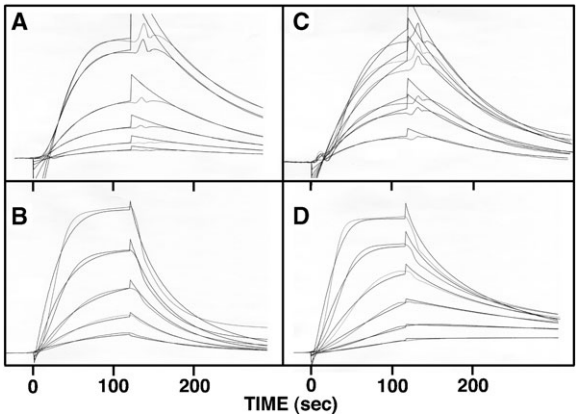

Fig. 7. The model fittings overlaid with the sensorgrams for the binding of FGF-2 to *Xenopus* HS chains. The fitting models were simulated by BIAevaluation 3.1 software and overlaid with the sensorgrams for the binding of FGF-2 to *Xenopus* embryonic HS chains prepared at the preMBP (**A**), gastrula (**B**), neurula (**C**), and taibud (**D**) stages.

the neurula to the tailbud stage resulted in a faster association of these growth factors with the *Xenopus* HS as well as a faster dissociation from the *Xenopus* HS. These results indicate that, even if there is no change in the value of K_d, alterations to binding parameters, namely the k_a and k_d values, can have a substantial biological impact.

Comparison of the affinity of growth factors for Xenopus CS/DS preparations at different developmental stages

The K_d value for the interaction of FGF-2 or PTN with the *Xenopus* CS/DS decreased or increased with development as follows: 170 or 3.3 (gastrula), 14 or 6.8 (neurula), and 0.75 or 22 nM (tailbud), respectively (Table IV and Figure 8). As the embryogenesis proceeds, the structure of the CS/DS chains in *Xenopus* embryos undergoes a controlled gradual change to acquire or lose the ability to bind FGF-2 or PTN, respectively. In contrast, the K_d value observed for the interaction of MK with the *Xenopus* CS/DS altered with development as follows: 340 (gastrula), 1.0 (neurula), and 1.9 nM (tailbud), indicating that the affinity of the *Xenopus* CS/DS for MK increased by approximately 300-fold from the gastrula to the neurula stage, and then was retained until the tailbud stage.

Discussion

Several secreted growth factors including MK/PTN, the FGF family, and the transforming growth factor-β superfamily govern the formation of complex body structures and patterns during development. The distribution of these signaling molecules is regulated spatiotemporally. Studies with model animals have demonstrated the crucial roles of PGs in these signaling pathways during development (Perrimon and Bernfield 2000; Lin 2004). PG molecules regulate the activities and distribution of these signaling molecules by interacting through their GAG

Table III. Kinetic parameters for the interaction of FGF-2, MK, and PTN with immobilized *Xenopus* HS

Growth factors and developmental stages	k_a (M^{-1} S^{-1})	k_d (S^{-1})	K_d (nM)
Growth factor: FGF-2			
Pre-MBT	$(9.6 \pm 3.2) \times 10^5$	$(7.5 \pm 0.27) \times 10^{-3}$	8.9 ± 3.2
Gastrula	$(3.2 \pm 0.40) \times 10^4$	$(2.3 \pm 0.83) \times 10^{-2}$	760 ± 360
Neurula	$(8.9 \pm 3.4) \times 10^4$	$(9.6 \pm 0.12) \times 10^{-3}$	130 ± 51
Tailbud	$(1.3 \pm 0.31) \times 10^6$	$(6.8 \pm 3.4) \times 10^{-2}$	61 ± 40
Growth factor: MK			
pre-MBT	$(2.6 \pm 0.73) \times 10^5$	$(9.5 \pm 0.71) \times 10^{-5}$	0.41 ± 0.15
Gastrula	$(8.3 \pm 3.6) \times 10^4$	$(5.1 \pm 0.53) \times 10^{-6}$	0.080 ± 0.041
Neurula	$(1.2 \pm 0.26) \times 10^5$	$(4.9 \pm 2.1) \times 10^{-4}$	4.9 ± 2.9
Tailbud	$(3.1 \pm 0.98) \times 10^5$	$(1.4 \pm 0.51) \times 10^{-5}$	0.057 ± 0.034
Growth factor: PTN			
pre-MBT	$(2.5 \pm 0.67) \times 10^5$	$(9.2 \pm 0.19) \times 10^{-5}$	0.40 ± 0.12
Gastrula	$(4.2 \pm 0.65) \times 10^5$	$(3.4 \pm 2.8) \times 10^{-5}$	0.094 ± 0.081
Neurula	$(1.8 \pm 0.51) \times 10^5$	$(1.2 \pm 0.14) \times 10^{-4}$	0.74 ± 0.28
Tailbud	$(7.8 \pm 2.3) \times 10^5$	$(9.0 \pm 3.2) \times 10^{-4}$	1.4 ± 0.82

The k_a, k_d, and K_d values were determined using the "fit kinetics simultaneous k_a/k_d" program. The values are expressed as the mean ± SD.

chains. In the present study, the structural and functional alteration of GAG chains derived from *Xenopus* embryos at different stages of development was investigated.

Although the exact biological significance of the developmental changes in the sulfation profile remains to be investigated, they appear to affect at least some developmentally important events such as cellular adhesion, migration, and neurite outgrowth (Herndon and Lander 1990; Faissner et al. 1994; Sugahara and Mikami 2007). Nurcombe et al. (1993) reported that the HS-PG produced by the murine neuroepithelium at embryonic day 9 preferentially bound FGF-2 whereas there was a switch in the binding specificity of HS-PG to FGF-1 at embryonic day 11 concomitant with the temporal expression of the mRNA for FGFs. Brickman et al. (1998) demonstrated that the switch in the binding specificity of the murine neuroepithelial HS-PG from FGF-2 to FGF-1 depends on the alterations in sulfation patterns, total chain length, and the number of sulfated domains of the HS at the different developmental stages. Although such a clear discrete switch of the binding properties to growth factors as observed during murine neural development was not detected for *Xenopus* here, we demonstrated that the affinity for four different growth factors significantly varied during development. The structural changes of *Xenopus* GAGs appear to control the activities and functions of various growth/differentiation factors during embryogenesis.

The disaccharide composition of GAGs in *Xenopus* embryos altered during development (Figure 3). The degree to which *Xenopus* HS chains were sulfated gradually decreased with development. The proportion of nonsulfated disaccharide units increased but that of highly sulfated disaccharides decreased. However, the fine saccharide sequences in HS chains required for binding to growth factors seem to be formed even at the later stage of the *Xenopus* development because all the *Xenopus* HS chains showed significant affinity to growth factors tested.

The 4-sulfation of GalNAc residues was predominant in CS/DS chains from pre-MBT embryos (79%), but the ratio of ΔDi-6S to ΔDi-4S decreased gradually with development. At the tailbud stage, the GalNAc 6-sulfate-containing unit becomes the predominant disaccharide unit (44%). Previous studies have indicated that the ratio of 6-sulfation/4-sulfation of GalNAc residues in CS chains changes during the development of chick cartilage (Robinson and Dorfman 1969), chick brain (Kitagawa et al. 1997), rat skin (Habuchi et al. 1986), mouse brain (Maeda et al. 2003; Mitsunaga et al. 2006), pig brain (Bao et al. 2004), and human cartilage (Mathews and Glagov 1966). These studies showed that the ratio of ΔDi-6S to ΔDi-4S increased gradually during development in birds and mammals. The downregulation of the expression of the GalNAc 6-sulfate structure in chicken embryonic brain and mouse brain was found to be parallel the developmental expression of the chondroitin 6-sulfotransferase

Table IV. Kinetic parameters for the interaction of FGF-2, MK, and PTN with immobilized *Xenopus* CS/DS

Growth factors and developmental stages	k_a (M^{-1} S^{-1})	k_d (S^{-1})	K_d (nM)
Growth factor: FGF-2			
Gastrula	$(6.3 \pm 2.7) \times 10^4$	$(7.7 \pm 2.0) \times 10^{-3}$	170 ± 100
Neurula	$(3.6 \pm 1.4) \times 10^5$	$(4.3 \pm 0.37) \times 10^{-3}$	14 ± 6.7
Tailbud	$(1.5 \pm 0.69) \times 10^7$	$(6.7 \pm 4.0) \times 10^{-3}$	0.75 ± 0.63
Growth factor: MK			
Gastrula	$(4.5 \pm 2.9) \times 10^3$	$(7.0 \pm 2.6) \times 10^{-4}$	340 ± 280
Neurula	$(1.5 \pm 0.69) \times 10^5$	$(1.2 \pm 0.11) \times 10^{-4}$	1.0 ± 0.55
Tailbud	$(1.5 \pm 0.92) \times 10^5$	$(1.5 \pm 0.52) \times 10^{-4}$	1.9 ± 1.5
Growth factor: PTN			
Gastrula	$(1.7 \pm 0.21) \times 10^5$	$(5.0 \pm 3.0) \times 10^{-4}$	3.3 ± 2.3
Neurula	$(4.3 \pm 0.84) \times 10^4$	$(2.7 \pm 0.42) \times 10^{-4}$	6.8 ± 2.3
Tailbud	$(3.8 \pm 1.8) \times 10^4$	$(5.5 \pm 2.3) \times 10^{-4}$	22 ± 16

The k_a, k_d, and K_d values were determined using the "fit kinetics simultaneous k_a/k_d" program. The values are expressed as the mean ± SD.

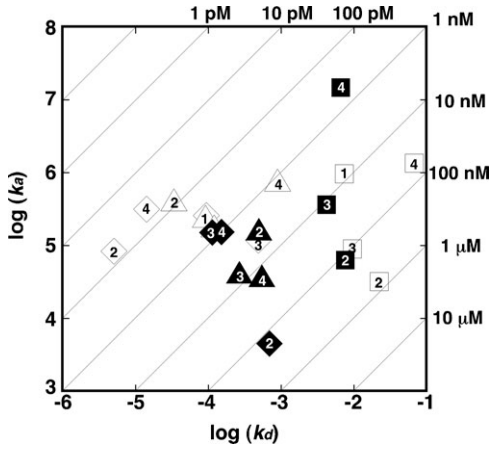

Fig. 8. The kinetic characteristics of *Xenopus* HS and CS/DS in their interactions with various growth factors. The interaction kinetic maps show the association versus dissociation rate constants (k_a and k_d, respectively) and the combination of k_a and k_d that results in the same K_d values (diagonal lines). Open symbols, HS; closed symbols, CS/DS. Squares, FGF-2; diamonds, MK; triangles, PTN. Numbers in the symbols indicate the developmental stage of *Xenopus* embryos: (1) pre-MBT; (2) gastrula; (3) neurula; (4) tailbud.

gene (Kitagawa et al. 1997; Mitsunaga et al. 2006). The 4-sulfation and 6-sulfation of CS chains on phosphacan PG also change during the development of the brain in rats (Margolis and Margolis 1993; Maeda et al. 1995). Substantial amounts of GalNAc 6-sulfate are found on phosphacan PG in the early developmental stages, but later, the CS chains of phosphacan PG are virtually composed of only GalNAc 4-sulfate structure. However, the results obtained in the present study are quite different. The ratio of ΔDi-6S to ΔDi-4S decreased gradually during *Xenopus* development. This inconsistency might be due to the difference in the expression pattern of sulfated structures of CS/DS among species or organs. Although whole embryos were used for the GAG structural analysis in this study, individual organs such as brain, skin, and cartilage were used in previous studies.

Apparently, the alteration of the affinity of GAGs for growth factors during development was not directly correlated with the change in the total amount or disaccharide composition of GAGs. These results indicated that the mechanism by which the affinity is altered during development is rather complicated, and that the expression of a certain saccharide sequence specifically interacting with a growth factor might be regulated during development.

Since *Xenopus* proteins were not commercially available, all growth/differentiation factors used in this study were human recombinant counterparts. The homology of amino acid sequences of FGF-2, MK, and PTN between *Xenopus* and human proteins are 84, 65, and 87%, respectively. No *Xenopus* ortholog for FGF-1 has been reported. Thus, the interaction between human FGF-1 and *Xenopus* GAGs may not reflect the physiological events in *Xenopus* embryogenesis. FGF-1 was used as a probe to detect the fine structural alteration of a special saccharide sequence interacting with FGF-1. At least the alteration of the fine structure of *Xenopus* GAGs during development has been demonstrated. In the future, an interaction analysis using *Xenopus* proteins will be required.

In this study, we detected high affinity of the *Xenopus* CS/DS for FGF-1. Although high affinity of HS for FGF-1 has been shown (Pellegrini 2001), strong binding between FGF-1 and CS/DS chains has never been reported to our knowledge. Previously highly sulfated CS/DS chains from squid cartilage, shark skin, hagfish notochord, or shark liver were subjected to an analysis of interaction with FGF-1 (Deepa et al. 2002; Nandini et al. 2004, 2005; Li et al. 2007). However, no CS/DS preparations showed affinity for FGF-1. Hence, the observation made in this study suggests the presence of a unique saccharide sequence in the *Xenopus* CS/DS chains, which specifically interacts with FGF-1. To characterize the FGF-1-binding structure in the CS/DS chains, inhibition experiments were carried out. Various CS/DS isomers were added as inhibitors mixed with FGF-1 to the BIAcore sensor chip on which the CS/DS preparation from the *Xenopus* tailbud embryos was immobilized. DS from bovine skin effectively inhibited the interaction of FGF-1 with the sensor's surface (results not shown), indicating that the DS-like structure in *Xenopus* CS/DS from the tailbud embryos is involved in the binding of FGF-1. The presence of the DS structure was demonstrated in the *Xenopus* CS/DS preparations from all the embryonic stages used (Table II). *Xenopus* CS/DS does not contain highly sulfated disaccharide units but is composed of only nonsulfated and monosulfated disaccharide units. Hence, the mixed sequence of CS with DS seems to be important to bind with FGF-1. The critical role of DS domains in neurite outgrowth has been reported (Bao et al. 2004, 2005; Nandini et al. 2005; Li et al. 2007). Decoding the DS-containing saccharide sequence, which specifically interacts with FGF-1, remains to be accomplished.

During the association phase of MK and PTN with *Xenopus* GAGs, the association curves showed virtually straight lines rather than exponential curves (Figures 5 and 6). A laminar flow system such as BIAcore instrument has a difficulty in measuring k_a values that are above 10^6 M^{-1} S^{-1}. The straight line association of MK and PTN for *Xenopus* GAGs may result from this fundamental limitation of a laminar flow system. The k_a values of PTN with *Xenopus* GAGs obtained in this study are approximately 10-fold lower than that with heparin measured by other group (1.6×10^6 M^{-1} S^{-1}) (Vacherot et al. 1999). They were rather similar to that of a fragment of PTN with heparin reported by Hamma-Kourbali et al. (2008) (3.4×10^5 M^{-1} S^{-1}), which binds less potently to heparin than the full-length PTN. The degree of sulfation of *Xenopus* GAGs (0.48–1.14 sulfate groups/disaccharide) (Table I and II) is much lower than that of heparin (approximately 2.6 sulfate groups/disaccharide) (Sugahara et al. 1992). Generally heparin has higher affinity to growth factors than less sulfated GAGs. Weaker association of the full-length PTN with *Xenopus* GAGs than heparin is reasonable, and the k_a values of PTN with *Xenopus* GAGs seem to be moderate. However, we cannot exclude the possibility of underestimation for the k_a values of PTN with *Xenopus* GAGs because of the fundamental limitation of the BIAcore system.

Although all growth factors tested showed small K_d values for the interaction with *Xenopus* GAGs, k_a and k_d values were distinct among growth factors. The interactions of *Xenopus* GAGs with MK and PTN have much smaller k_d values than those with FGF-2. As shown in Figure 8, spots for the interaction between *Xenopus* GAGs and MK or PTN (diamonds and triangles) are accumulated on the left side compared to those of FGF-2

(squares). A small k_d value indicates a slow dissociation of interaction and a stable binding. The strong association of MK or PTN with *Xenopus* GAGs and the negligible dissociation from *Xenopus* GAGs prompted us to speculate that MK or PTN is not released as a free signaling molecule, but rather enzymatically released as a growth factor–GAG complex from a parent PG molecule by endoglycosidases, such as hyaluronidase and heparanase, and transferred to the cell-surface receptor. Recently *Xenopus* heparanases have been demonstrated to be necessary in early embryonic development (Bertolesi et al. 2008). In contrast, the interaction of *Xenopus* GAGs with FGF-2 showed large k_a and k_d values, indicating that these growth factors bind to and separate from *Xenopus* GAGs quickly. Hence, FGFs are readily transferred from *Xenopus* GAGs to the cell-surface receptors without cleavage by glycosidases, and *Xenopus* GAGs may function as coreceptors of FGFs.

The difference in affinity for various growth/differentiation factors between the *Xenopus* HS and CS/DS at the same developmental stage was investigated. When the positions of the same numbered and shaped symbols are compared in Figure 8, open diamonds (MK) and triangles (PTN) are always to the upper left of closed ones but closed squares (FGF-2) are always located to the upper left of open ones, indicating that FGF-2 showed higher affinity for *Xenopus* CS/DS than HS whereas MK and PTN showed higher affinity for *Xenopus* HS than CS/DS at all the developmental stages examined. The high affinity of FGFs for CS/DS was unexpected because to our knowledge, no reports have demonstrated stronger binding of CS/DS chains to FGFs than HS from the same source. The disaccharide composition of *Xenopus* CS/DS is not striking because of the lack of highly sulfated units, which have been demonstrated to play important roles in the functions of CS/DS in neurite outgrowth and immune system (Kawashima et al. 2002; Nandini et al. 2004; Mitsunaga et al. 2006; Sotogaku et al. 2007). However, *Xenopus* CS/DS chains contain a significant proportion of DS domain. The mixed sequence composed of CS with DS may be responsible for the high affinity to FGFs. Accumulating evidence demonstrates the important functions of DS domains in neurite outgrowth through interactions with growth/differentiation factors (Bao et al. 2004, 2005; Nandini et al. 2005; Li et al. 2007). Although the physiological significance of the high affinity of CS/DS chains for FGFs remains to be clarified due to the use of human recombinant proteins, the strong affinity of CS/DS for FGFs may be significant and CS/DS chains also may play indispensable roles during *Xenopus* embryogenesis.

Material and methods

Materials

Heparitinase (EC 4.2.2.8), heparinase (EC 4.2.2.7), chondroitinase ABC (EC 4.2.2.4), AC-I (EC 4.2.2.5), AC-II (EC 4.2.2.5), and B (EC 4.2.2), unsaturated disaccharides derived from CS/DS, and various CS isoforms were obtained from Seikagaku Corp., Tokyo, Japan. 2AB was purchased from Nacalai Tesque, Kyoto, Japan. Unsaturated disaccharides derived from heparin and HS were prepared as described (Yamada et al. 1992). Eggs of general *X. laevis* at the pre-MBT, gastrula, neurula, and tailbud stages were prepared as described (Nieuwkoop and Faber 1956).

Preparation of the GAG chains from Xenopus embryos

Xenopus embryos at different developmental stages (9–12 mL) were homogenized in ice-cold acetone. The homogenates were filtrated, extracted with chloroform/methanol/water (5:5:1), and air-dried. Approximately 2.2, 2.3, 1.3, and 1.5 g of the dried materials were recovered from 10 mL of *Xenopus* embryos at the pre-MBT, gastrula, neurula, and tailbud stages, respectively. These samples were exhaustively digested with actinase E (Kaken Pharmaceutical Co., Tokyo) at 60°C for 48 h, and then the acid soluble fraction (5% trichloroacetic acid) was extracted with ether, and the aqueous phase was adjusted to 80% ethanol (Yamada et al. 2002). The resultant precipitate was dissolved in the 0.15 M LiCl/50 mM sodium acetate buffer, pH 4.0, and applied to a column of DEAE-cellulose (Amersham Pharmacia Biotech, Uppsala, Sweden). After a wash with the starting buffer, stepwise elution was conducted with buffers containing 0.5, 1.0, and 1.5 M LiCl. The hexuronic acid in each fraction was quantified by the carbazole method, using D-glucuronic acid as a standard (Bitter and Muir 1962). The flow-through and 1.5 M LiCl-eluted fractions did not contain GAGs. The fractions eluted with 0.5 and 1.0 M LiCl were used for further analysis. HPLC analysis after enzymatic digestion as described below indicated that more than 90% of the sulfated GAGs were recovered in 1.0 M LiCl-eluted fractions, which were used for the examination of the interactions with growth factors.

Enzymatic treatments and HPLC analysis

Enzymatic treatments for the disaccharide composition analysis were carried out as follows. An aliquot of a GAG fraction (8–280 mg as the dried materials) was digested with chondroitinase ABC (10 mIU) in a total volume of 50 μL of 0.05 M Tris-HCl buffer, pH 8.0, containing 0.06 M sodium acetate at 37°C for 30 min, with chondroitinase AC-I (10 mIU) or a mixture of chondroitinases ABC and AC-I (5 mIU each) in a total volume of 50 μL of 0.05 M Tris-HCl buffer, pH 7.3, at 37°C for 30 min, or with a mixture of heparinase and heparitinase (2 mIU each) in a total volume of 50 μL of acetate-NaOH buffer, pH 7.0, containing 10 mM $Ca(OAc)_2$ at 37°C for 2 h. The digests were labeled with a fluorophore 2AB and analyzed by HPLC on an amine-bound silica column as reported previously (Kinoshita and Sugahara 1999).

Gel filtration chromatography of Xenopus GAGs

To determine the chain length of polysaccharides, the *Xenopus* GAG fraction was analyzed by gel filtration HPLC on a column (10 × 300 mm) of Superdex 200 eluted with 0.2 M ammonium bicarbonate at a flow rate of 0.4 mL min^{-1}. Fractions were collected at 2.0 min intervals, lyophilized, and digested with chondroitinase ABC or a mixture of heparinase and heparitinase. The digests were derivatized with 2AB, and then analyzed by HPLC on an amine-bound PA-03 column (Kinoshita and Sugahara 1999).

Preparation of biotinylated Xenopus GAGs

Xenopus GAG fractions were biotinylated as previously reported for heparin and CS-E preparations (Deepa et al. 2002). The weight ratio of GAGs to biotin-LC-hydrazide and 1-ethyl-3-[3-dimethylaminopropyl]carbodiimide hydrochloride reagents was approximately 3:1:1.

Growth factor-binding assays using a BIAcore system

Real-time analysis of the interactions of growth factors with biotinylated *Xenopus* GAG fractions or their digests with GAG lyases was performed with a BIAcore™ J biosensor (BIAcore AB, Uppsala, Sweden). A streptavidin-coated sensor chip was used to immobilize the biotinylated samples. Comparable amounts of samples were used for immobilization. The injection of biotinylated samples onto the sensor's surface was controlled to obtain a response of 320–570 resonance units (RU). BIAcore J uses a dual-channel flow and detection system so that one channel may be used as an in-line reference for sample analysis, to enhance the specificity of analyte detection. The principle of an in-line reference cell is that the sample cell is prepared with a ligand, to which the analyte binds, whereas the reference cell is either left unmodified or coated with a protein, to which the analyte does not bind. Subtracting the reference from the sample response thus gives the ligand-specific response. For the analysis of *Xenopus*–HS-specific interactions, the reference cell was prepared with biotinylated *Xenopus* GAG fractions treated with a mixture of heparinase and heparitinase. For the analysis of *Xenopus*–CS/DS-specific interactions, the sample cell was prepared with biotinylated *Xenopus* GAG fractions treated with a mixture of heparinase and heparitinase, and the corresponding reference cell was immobilized with the double digests of biotinylated *Xenopus* GAG fractions with chondroitinase ABC as well as a mixture of heparinase and heparitinase. The conditions for the kinetic analysis were the same as those reported previously (Deepa et al. 2004; Bao et al. 2005). The kinetic parameters, namely the association rate constant (k_a), the dissociation rate constant (k_d), and the equilibrium dissociation constant (K_d), were calculated wth BIAevaluation 3.1 software (BIAcore AB, Uppsala, Sweden) using a 1:1 binding model with mass transfer.

An interaction study using GAG in surface measurement always has an issue of rebinding which prevent calculating the intrinsic k_d values (Sadir et al. 1998). When measuring the binding of a protein factor to whole GAG chains, the protein may dissociate from one site on a chain and then rebind further along the chain. Such rebinding may artifactually reduce the measured value. Thus, it should be noted that some of the measurements shown in Figures 5 and 6 might be suffering from rebinding.

Supplementary Data

Supplementary data for this article is available online at http://glycob.oxfordjournals.org/.

Funding

The Japan Private School Promotion Foundation (HAITEKU, 2004–2008); the Ministry of Education, Culture, Sports, Science and Technology of Japan (Scientific Research C-19590052 to S.Y. and Scientific Research B-20390019 to K.S.); and the Human Frontier Science Program (RGP0018/2005 to K.S.).

Conflict of interest statement

None declared.

Abbreviations

2AB, 2-aminobenzamide; 2S, 2-*O*-sulfate; 6S, 6-*O*-sulfate; CS, chondroitin sulfate; DS, dermatan sulfate; FGF, fibroblast growth factor; GAG, glycosaminoglycan; GlcNS, *N*-sulfated glucosamine; HS, heparan sulfate; MBT, midblastula transition; MK, midkine; PTN, pleiotrophin; RU, resonance unit; ΔHexUA, 4-deoxy-α-L-*threo*-hex-4-enepyranosyluronic acid; ΔDi-0S, ΔHexUAα1-3GalNAc; ΔDi-4S, ΔHexUAα1-3GalNAc(4-sulfate); ΔDi-6S, ΔHexUAα1-3GalNAc(6-sulfate); ΔDi-diS_D, ΔHexUA(2-sulfate)α1-3GalNAc (6-sulfate); ΔDi-diS_E, ΔHexUAα1-3GalNAc(4,6-disulfate); ΔDi-triS, ΔHexUA(2-sulfate)α1-3GalNAc(4,6-disulfate).

References

Amaya E, Musci TJ, Kirschner MW. 1991. Expression of a dominant negative mutant of the FGF receptor disrupts mesoderm formation in *Xenopus* embryos. *Cell.* 66:257–270.

Bao X, Mikami T, Yamada S, Faissner F, Muramatsu T, Sugahara K. 2005. Heparin-binding growth factor, pleiotrophin, mediates neuritogenic activity of embryonic pig brain-derived chondroitin sulfate/dermatan sulfate hybrid chains. *J Biol Chem.* 280:9180–9191.

Bao X, Nishimura S, Mikami T, Yamada S, Itoh N, Sugahara K. 2004. Chondroitin sulfate/dermatan sulfate hybrid chains from embryonic pig brain, which contain a higher proportion of L-iduronic acid than those from adult pig brain, exhibit neuritogenic and growth factor binding activities. *J Biol Chem.* 279:9765–9776.

Bergefall K, Trybala E, Johansson M, Uyama T, Naito S, Yamada S, Kitagawa H, Sugahara K, Bergström T. 2005. Chondroitin sulfate characterized by the E-disaccharide unit is a potent inhibitor of herpes simplex virus infectivity and provides the virus binding sites on gro2C cells. *J Biol Chem.* 280:32193–32199.

Bertolesi GE, Michaiel G, McFarlane S. 2008. Two heparanase splicing variants with distinct properties are necessary in early *Xenopus* development. *J Biol Chem.* 283:16004–16016.

Bitter M, Muir H. 1962. A modified uronic acid carbazole reaction. *Anal Biochem.* 4:330–334.

Brickman MC, Gerhart JC. 1994. Heparitinase inhibition of mesoderm induction and gastrulation in *Xenopus laevis* embryos. *Dev Biol.* 164:484–501.

Brickman YG, Ford MD, Gallagher JT, Nurcombe V, Bartlett PF, Turnbull JE. 1998. Structural modification of fibroblast growth factor-binding heparan sulfate at a determinative stage of neural development. *J Biol Chem.* 273:4350–4359.

Conrad HE. 1998. *Heparin-Binding Proteins*. San Diego (CA): Academic.

Deepa SS, Umehara Y, Higashiyama S, Itoh N, Sugahara K. 2002. Specific molecular interactions of oversulfated chondroitin sulfate E with various heparin-binding growth factors. Implications as a physiological binding partner in the brain and other tissues. *J Biol Chem.* 277:43707–43716.

Deepa SS, Yamada S, Zako M, Goldberger O, Sugahara K. 2004. Chondroitin sulfate chains on syndecan-1 and syndecan-4 from normal murine mammary gland epithelial cells are structurally and functionally distinct and cooperate with heparan sulfate chains to bind growth factors. A novel function to control binding of midkine, pleiotrophin, and basic fibroblast growth factor. *J Biol Chem*. 279:37368–37376.

Faissner A, Clement A, Lochter A, Streit A, Mandl C, Schachner M. 1994. Isolation of a neural chondroitin sulfate proteoglycan with neurite outgrowth promoting properties. *J Cell Biol.* 126:783–799.

Fujita N, Nagata S. 2005. Repulsive guidance of axons of spinal sensory neurons in *Xenopus laevis* embryos: Roles of Contactin and notochord-derived chondroitin sulfate proteoglycans. *Dev Growth Differ.* 47:445–456.

Furuya S, Sera M, Tohno-oka R, Sugahara K, Shiokawa K, Hirabayashi Y. 1995. Elimination of heparan sulfate by heparitinases induces abnormal mesodermal and neural formation in *Xenopus* embryos. *Dev Growth Differ.* 37:337–346.

Habuchi H, Kimata K, Suzuki S. 1986. Changes in proteoglycan composition during development of rat skin. The occurrence in fetal skin of a chondroitin sulfate proteoglycan with high turnover rate. *J Biol Chem*. 261:1031–1040.

Hamma-Kourbali Y, Bernard-Pierrot I, Heroult M, Dalle S, Caruelle D, Milhiet PE, Fernig DG, Delbé J, Courty J. 2008. Inhibition of the mitogenic, angiogenic and tumorigenic activities of pleiotrophin by a synthetic peptide corresponding to its C-thrombospondin repeat-I domain. *J Cell Physiol.* 214:250–259.

Herndon ME, Lander AD. 1990. A diverse set of developmentally regulated proteoglycans is expressed in the rat central nervous system. *Neuron*. 4:949–961.

Hou S, Maccarana M, Min TH, Strate I, Pera EM. 2007. The secreted serine protease xHtrA1 stimulates long-range FGF signaling in the early *Xenopus* embryo. *Dev Cell.* 13:226–241.

Itoh K, Sokol SY. 1994. Heparan sulfate proteoglycans are required for mesoderm formation in *Xenopus* embryos. *Development.* 120:2703–2711.

Kawashima H, Atarashi K, Hirose M, Hirose J, Yamada S, Sugahara K, Miyasaka M. 2002. Oversulfated chondroitin/dermatan sulfates containing GlcAβ1/IdoAα1-3GalNAc(4,6-*O*-disulfate) interact with L- and P-selectin and chemokines. *J Biol Chem.* 277:12921–12930.

Kinoshita A, Sugahara K. 1999. Microanalysis of glycosaminoglycan-derived oligosaccharides labeled with a fluorophore 2-aminobenzamide by high-performance liquid chromatography: Application to disaccharide composition analysis and exosequencing of oligosaccharides. *Anal Biochem.* 269:367–378.

Kitagawa H, Tsutsumi K, Tone Y, Sugahara K. 1997. Developmental regulation of the sulfation profile of chondroitin sulfate chains in the chicken embryo brain. *J Biol Chem.* 272:31377–31381.

Li F, Shetty AK, Sugahara K. 2007. Neuritogenic activity of chondroitin/dermatan sulfate hybrid chains of embryonic pig brain and their mimicry from shark liver. Involvement of the pleiotrophin and hepatocyte growth factor signaling pathways. *J Biol Chem.* 282:2956–2966.

Lin X. 2004. Functions of heparan sulfate proteoglycans in cell signaling during development. *Development.* 131:6009–6021.

Maeda N, Hamanaka H, Oohira A, Noda M. 1995. Purification, characterization and developmental expression of a brain-specific chondroitin sulfate proteoglycan, 6B4 proteoglycan/phosphacan. *Neuroscience.* 67:23–35.

Maeda N, He J, Yajima Y, Mikami T, Sugahara K, Yabe T. 2003. Heterogeneity of the chondroitin sulfate portion of phosphacan/6B4 proteoglycan regulates its binding affinity for pleiotrophin/heparin binding growth-associated molecule. *J Biol Chem.* 278:35805–35811.

Margolis RK, Margolis RU. 1993. Nervous tissue proteoglycans. *Experientia.* 49:429–446.

Mathews MB, Glagov S. 1966. Acid mucopolysaccharide patterns in aging human cartilage. *J Clin Invest.* 45:1103–1111.

Mitsunaga C, Mikami T, Mizumoto S, Fukuda J, Sugahara K. 2006. Chondroitin sulfate/dermatan sulfate hybrid chains in the development of cerebellum. Spatiotemporal regulation of the expression of critical disulfated disaccharides by specific sulfotransferases. *J Biol Chem.* 281:18942–18952.

Nandini CD, Itoh N, Sugahara K. 2005. Novel 70-kDa chondroitin sulfate/dermatan sulfate hybrid chains with a unique heterogeneous sulfation pattern from shark skin, which exhibit neuritogenic activity and binding activities for growth factors and neurotrophic factors. *J Biol Chem.* 280:4058–4069.

Nandini CD, Mikami T, Ohta M, Itoh N, Akiyama-Nambu F, Sugahara K. 2004. Structural and functional characterization of oversulfated chondroitin sulfate/dermatan sulfate hybrid chains from the notochord of hagfish. Neuritogenic and binding activities for growth factors and neurotrophic factors. *J Biol Chem.* 279:50799–50809.

Nieuwkoop PD, Faber J. 1956. *Normal Table of Xenopus Laevis (Daudin)*. Amsterdam: North-Holland.

Nurcombe V, Ford MD, Wildschut JA, Bartlett PF. 1993. Developmental regulation of neural response to FGF-1 and FGF-2 by heparan sulfate proteoglycan. *Science.* 260:103–106.

Pellegrini L. 2001. Role of heparan sulfate in fibroblast growth factor signalling: A structural view. *Curr Opin Struct Biol.* 11:629–634.

Perrimon N, Bernfield M. 2000. Specificities of heparan sulphate proteoglycans in developmental processes. *Nature.* 404:725–728.

Robinson HC, Dorfman A. 1969. The sulfation of chondroitin sulfate in embryonic chick cartilage epiphyses. *J Biol Chem*. 244:348–352.

Rodén L. 1998. Structure and metabolism of connective tissue proteoglycans. In: Lennarz WJ, editor. *The Biochemistry of Glycoproteins and Poteoglycans*. New York: Plenum. p. 267–371.

Sadir R, Forest E, Lortat-Jacob H. 1998. The heparan sulfate binding sequence of interferon-gamma increased the on rate of the interferon-gamma-interferon-gamma receptor complex formation. *J Biol Chem.* 273:10919–10925.

Sekiguchi K, Yokota C, Asashima M, Kaname T, Fan Q-W, Muramatsu T, Kadomatsu K. 1995. Restricted expression of *Xenopus* midkine gene during early development. *J Biochem.* 118:94–100.

Sive HL, Grainger RM, Harland RM. 2000. *Early Development of Xenopus Laevis*. Cold Spring Harbor, NY: Cold Spring Harbor Laboratory Press.

Song J, Slack JMW. 1994. Spatial and temporal expression of basic fibroblast growth factor (FGF-2) mRNA and protein in early *Xenopus* development. *Mech Dev.* 48:141–151.

Sotogaku N, Tully SE, Gama CI, Higashi H, Tanaka M, Hsieh-Wilson LC, Nishi A. 2007. Activation of phospholipase C pathways by a synthetic chondroitin sulfate-E tetrasaccharide promotes neurite outgrowth of dopaminergic neurons. *J Neurochem.* 103:749–760.

Sugahara K, Mikami T. 2007. Chondroitin/dermatan sulfate in the central nervous system. *Curr Opin Struct Biol.* 17:536–545.

Sugahara K, Yamada S, Yoshida K, de Waard P, Vliegenthart JF. 1992. A novel sulfated structure in the carbohydrate–protein linkage region isolated from porcine intestinal heparin. *J Biol Chem.* 267:1528–1533.

Tsuchida K, Shioi J, Yamada S, Boghosian G, Wu A, Cai H, Sugahara K, Robakis NK. 2001. Appican, the proteoglycan form of the amyloid precursor protein, contains chondroitin sulfate E in the repeating disaccharide region and 4-*O*-sulfated galactose in the linkage region. *J Biol Chem.* 276:37155–37160.

Tujimura K, Yasojima K, Kuboki Y, Suzuki A, Ueno N, Shiokawa K, Jashimoto-Goroh T. 1995. Developmental and differential regulations in gene expression of *Xenopus* pleiotrophic factors-alpha and -beta. *Biochem Biophys Res Commun.* 214:432–439.

Ueoka C, Kaneda N, Okazaki I, Nadanaka S, Muramatsu T, Sugahara K. 2000. Neuronal cell adhesion, mediated by the heparin-binding neuroregulatory factor midkine, is specifically inhibited by chondroitin sulfate E. Structural and functional implications of the over-sulfated chondroitin sulfate. *J Biol Chem.* 275:37407–37413.

Vacherot F, Delbé J, Heroult M, Barritault D, Fernig DG, Courty J. 1999. Glycosaminoglycans differentially bind HARP and modulate its biological activity. *J Biol Chem.* 274:7741–7747.

Yamada S, Okada Y, Ueno M, Iwata S, Deepa SS, Nishimura S, Fujita M, Van Die I, Hirabayashi Y, Sugahara K. 2002. Determination of the glycosaminoglycan–protein linkage region oligosaccharide structures of proteoglycans from *Drosophila melanogaster* and *Caenorhabditis elegans*. *J Biol Chem.* 277:31877–31886.

Yamada S, Yoshida K, Sugiura M, Sugahara K. 1992. One- and two-dimensional ^{1}H-NMR characterization of two series of sulfated disaccharides prepared from chondroitin sulfate and heparan sulfate/heparin by bacterial eliminase digestion. *J Biochem.* 112:440–447.